Astron. Astrophys. 319, 796–810 (1997)

ASTRONOMY
AND
ASTROPHYSICS

uvby-β photometry of high-velocity and metal-poor stars

IX. Effects of orbital chaos in the Galactic halo⋆

W.J. Schuster[1,2] **and Christine Allen**[2]

[1] Observatorio Astronómico Nacional, UNAM, Apartado Postal 877, C.P. 22800, Ensenada, B.C., México
[2] Instituto de Astronomía, UNAM, Apartado Postal 70-264, C.P. 04510, México, D.F., México

Received 2 April 1996 / Accepted 12 September 1996

Abstract. Galactic orbits have been integrated using the Galactic potential model of Allen & Santillán (1991) for 280 halo stars identified in the V_{rot}, [Fe/H] diagram. The effects of chaos upon their orbital structure have been investigated.

A "vertical" surface of section is defined, where Z is plotted versus z each time the orbit crosses the cylinder $\tilde{\omega}$ = 8.5 kpc; this surface of section allows a more complete visualization of the Galactic orbits in phase space, a better understanding of the orbital chaos, and a more direct comparison with observations. "Horizontal" surfaces of section and meridional orbits have also been plotted for all of these halo stars, and have been used to classify the Galactic orbits into the categories box, chaotic, and resonant; 44.3% of the halo orbits are found to show some evidence of chaos.

The observed $|W'|$ velocities of the halo stars give poor measures of z_{max} for the box orbits, and especially for the chaotic orbits. Regressions of [Fe/H] against R_{max} and z_{max}, for the total sample and for the chaotic and non-chaotic subsets, show little evidence for a metallicity gradient in the Galactic halo.

The surfaces of section for many of the halo stars ($\sim$ a third) show some evidence of structure within chaos. Part of this structure is due to the "stickiness" that chaotic orbits experience near the outer KAM tori of families of periodic and quasiperiodic orbits. This "stickiness" has been discussed extensively in the literature. The phase-space clumpiness produced by this "stickiness" may help to explain the "moving groups" found in the solar vicinity and the non-Gaussian velocity distributions observed at the Galactic poles. Also, the "confinement" of the chaotic orbits by a 1:1 resonant family of tube orbits, which passes a few kpc above the Sun, may explain part of the halo duality which has been detected in several studies, such as those of Hartwick (1987) and of Kinman et al. (1994).

Histograms of the observed $|W'|$ velocity and of the calculated orbital parameter z_{max} have been plotted for the 280 halo stars. Structure is seen in both histograms, due mainly to the chaotic orbits; the $|W'|$ histogram is non-Gaussian with two peaks, and the z_{max} histogram has three peaks. Remarkably the structure in these two histograms is correlated and can be explained in relation to the details of the surfaces of section and the "confinement" and "stickiness" phenomena of the chaotic orbits.

Key words: chaos – stars: kinematics – Galaxy: halo – Galaxy: kinematics and dynamics – Galaxy: structure

1. Introduction

In a pioneering work Hénon & Heiles (1964) investigated, via numerical experiments, the existence of a third isolating integral of motion for an axisymmetric potential and found that under certain conditions, such as higher energies, a considerable ergodic "sea" quickly developed in phase space. They also found evidence for a very intricate transition from families of closed orbits to chaos, such as infinitely dense islands and island chains and orbits "intermediate" between the quasiperiodic orbits and the chaotic ones. Such results gave some of the first hints concerning the possible importance of chaos to stellar and planetary dynamics.

In the intervening years the understanding and application of chaotic dynamics has grown considerably (for example, Ott 1993; Gurzadyan and Pfenniger 1994). In the astronomical realm, the theory of chaos has found very fruitful applications to solar system dynamics, as reviewed by Wisdom (1987). The chaotic tumbling of Hyperion (Wisdom et al. 1984) and the chaotic orbits of asteroids as an explanation for the Kirkwood gaps (Froeschlé & Scholl 1979, 1981; Wisdom 1983; Soper et al. 1990; Franklin et al. 1993; and Franklin 1994) are good examples. Also, Petit & Hénon (1986) found evidence for chaotic

Send offprint requests to: W.J. Schuster. P.O. Box 439027, San Diego, CA, 92143-9027, USA

⋆ Based on observations collected at the Observatorio Astronómico Nacional at San Pedro Mártir, Baja California, México, and at the Danish telescopes, La Silla, Chile.

effects within satellite encounters, and Laskar (1989) has shown that the inner solar system, including the Earth's orbit, is chaotic.

On a larger scale observational and theoretical evidence has been mounting that chaos may play an important role in the stellar dynamics of halo stars within our Galaxy. Grenon (1987, 1989) claims that a high percentage of metal-deficient stars have chaotic orbits, with the angular moment of the orbits being the crucial parameter. Stars with $|V_{rot}| < 50$ km s^{-1} or $R_{peri} < 0.7$ kpc most likely have stochastic orbits, where V_{rot} is the star's rotational velocity about the Galactic center and R_{peri}, the perigalactic distance of the orbit. In their study of the halo metallicity gradient, Carney et al. (1990a) never use the words "chaos", "stochasticity", nor "ergodicity", but mention that "stars... that pass too near the central mass may have their radial and vertical motions mixed". The increasing criteria used to filter the halo stars of their Fig. 11 are essentially criteria to remove the stars with the more chaotic orbits, criteria such as $|U| \leq 130$ km s^{-1}, $R_{apo} \leq 12$ kpc and $R_{peri} \geq 1$ kpc, where U is the radial Galactic velocity, R_{apo} is the apogalactic distance reached in the stellar orbit, and R_{peri}, as above. Their Fig. 11 analyzes the correlation of $|Z_{max}|$ with $|W|$, where Z_{max} is the maximum distance above or below the Galactic plane reached in a star's orbit and $|W|$ the vertical velocity in the solar neighborhood. They find generally little correlation between $|Z_{max}|$ and $|W|$ for their full sample but increasing correlation as the stars with chaotic orbits are removed.

Allen et al. (1991; hereafter Paper IV) calculate Galactic orbits for a sample of 43 halo stars with [Fe/H] ≤ -2.0 using the Galactic potential of Allen & Martos (1986). They classify the orbits as "box", "tube", or "chaotic" using meridional-orbit projections and surfaces of section (as defined below), and find $\sim 28\%$ chaotic orbits. Allen et al. note that this chaos results for halo stars with low orbital angular momenta which visit the central kiloparsec of the Galaxy, "... the force exerted by the spherical mass distribution becomes dominant, and this will tend to randomize the orbit". They comment that such chaos will produce noise upon the studies of chemical gradients within the Galactic halo.

Valera et al. (1994a,b) calculated Galactic orbits for the same 280 halo stars being analyzed in this paper, using three different Galactic potentials, those of Allen & Santillán (1991), of Bahcall et al. (1982, 1983), and of Caldwell & Ostriker (1983). Only surfaces of section were used for the orbital classifications, but $\sim 40\%$ of the orbits were found to be chaotic, independent of the model. The numbers of box and resonant orbits were found to decrease sharply for R_{peri}'s inside 1 kpc and the number of chaotic orbits to increase sharply. $\langle R_{peri} \rangle$ ~0.2-0.3 kpc for the chaotic orbits. It was concluded that the spherical bulge or central-mass components of these potentials "scatter" stars penetrating the inner 1 kpc, leading to the chaotic behavior. In the $|z_{max}|$ histrograms the chaotic component of the halo stars produces a peak at about 5-7 kpc due to this "scattering" and due to their dominance by the spherical components of the Galaxy (bulge plus halo), while the halo stars with box orbits produce a peak in the Galactic plane ($|z_{max}| \lesssim 1.5$ kpc) due to their dominance by the disk (axisymmetric) components of the potentials.

Congruently, Hartwick (1987), and more recently Kinman et al. (1994), have found evidence for a two-component halo using the space distributions of metal-poor RR Lyrae variables and blue horizontal branch stars. They find an inner flattened component (c/a ~ 0.6) with a scale height in the range $\sim 1.6 - 2.2$ kpc and an outer, nearly spherical, component. The similar [Fe/H] distributions of these two subsets seem to rule out a dissipative collapse for the formation of the inner component, and Hartwick (1987) concludes, "... the dominant flattening mechanism is due to the dynamical evolution of an extant population of stars and clusters ..."

In this paper Galactic orbits are calculated and analyzed in detail for the 280 halo stars from Schuster, Parrao and Contreras-Martínez (1993; hereafter SPC) using the Galactic mass model of Allen & Santillán (1991), with photometric distances from the calibration of Nissen & Schuster (1991; Paper V) forming part of the initial conditions for the orbital integrations. The values of E(b-y) and [Fe/H] for individual halo stars, necessary for accurate distances, have been derived using the calibrations of Paper II (Schuster & Nissen 1989a). Other papers in this series, such as Schuster & Nissen (1989b; Paper III) and Marquez & Schuster (1994; Paper VII), have analyzed the ages of the halo and thick-disk field stars, including a possible radial gradient in the halo-star ages.

A careful look is taken at the correlations, or lack thereof, between z_{max} and $|W'|$ and between [Fe/H] and z_{max} or R_{max} for the halo stars. It is concluded that in general there is not a good correlation between z_{max} and $|W'|$ and that chaotic orbits tend to destroy the correlation even more. No obvious chemical gradient is found for the halo sample even when the stars with chaotic orbits have been removed.

Vertical and horizontal surfaces of section (Poincaré sections) are defined and used to analyze the phase-space structure of halo-star orbits, specially the "clumpiness", "clustering", "sticking", and/or "confinement" of the chaotic orbits by families of quasiperiodic or resonant orbits. Such structure is also seen as a double peak in our W' histogram, at -20 km s^{-1} and +60 km s^{-1}, and a triple peak in the z_{max} histogram, at 0.0-0.5 kpc, 1.5-2.0 kpc, and 5-7 kpc. Percentages are estimated, example orbits plotted for the various types of orbit and orbital interaction, and it is suggested that such phenomena may be responsible for the maintenance and/or production of some of the "moving groups" within the halo field stars, for the unusual velocity distributions observed at the Galactic poles and perhaps also for part of the vertical structure ("two-component model") observed for halo stars by Hartwick (1987) and by Kinman et al. (1994).

2. Methodology

2.1. Selection of the halo stars

The 280 halo stars analyzed in this paper were drawn from our two photometric catalogues, Schuster & Nissen (1988, here-

after SN) and SPC, which were based in large part on previous high-velocity and proper-motion catalogues, and so contain mainly a kinematic selection bias. The sources and biases of our photometric catalogues are discussed in greater detail in these previous two papers.

The separation of the halo stars from the other stellar populations has been carried out using the V_{rot}, [Fe/H] diagram, as described in Paper V and SPC. A diagonal cut in this diagram provides us with a nearly pure halo sample. In SPC it was shown that this halo sample probably contains fewer than about 6 contaminating thick-disk stars. Orbital integrations for 1153 stars from our two photometric catalogues have shown that such contaminating thick-disk stars should have non-chaotic, "box" orbits and so should not affect in any significant way the results to follow; the percentage of chaotic orbits among our stars, as compared to a pure halo sample, may be slightly underestimated.

On the other hand, the kinematic selection bias of our halo sample will cause us to over-estimate the percentage of chaotic orbits. As shown in Paper V and in Carney et al. (1990b) the U'-velocity dispersion of our selected halo sample suffers much more severely from the kinematic bias than do the dispersions in V' and W'. Our kinematically selected halo sample will contain a higher percentage of center-passing Galactic orbits than would a non-kinematically selected sample.

2.2. Previous photometric calibrations and kinematic data

The values of E(b-y) and [Fe/H] used in these analyses have been derived using the intrinsic-color and metallicity calibrations of Paper II. The procedures for de-reddening the photometry are given in Papers II and III. The photometric distances have been calculated using the calibration of Paper V, which includes an evolutionary correction of the form, $\delta M_v = f\delta c_0$, where the f coefficient is taken from Nissen et al. (1987), and δc_0 is the displacement of a star in the c_0, $(b-y)_0$ diagram from its corresponding ZAMS.

The radial velocities and proper motions used to calculate the initial conditions of the orbital integrations were taken from many sources, as described in Papers V and SPC. The standard deviations of the observed radial velocities range from less than 1 km s^{-1} for sources such as Carney & Latham (1987) to $\lesssim$ 10 km s^{-1} for sources such as Norris et al. (1985). Typical errors in μ_α and μ_δ fall in the range 0.″01 to 0.″03 yr^{-1}. An attempt was made to select always the most reliable and most accurate values, or an average value if several equally reliable sources were available. Representative errors of the stars' total space velocities lie in the range 10 to 30 km s^{-1}; for most halo stars, the largest contribution to this error arises from the uncertainty of the distance determination. In a few cases such errors are sufficient to change the orbital classifications of the individual halo stars and the structure of the chaotic orbits, but should not change significantly the global, ensemble results for our 280 halo stars.

The computer program for calculating the space velocities, (U', V', W'), or the cylindric Galactocentric velocities (Π, Z, Θ) is based on the precepts and equations of Johnson & Soderblom (1987). The adopted corrections for the solar motion are $(-10.0, +14.9, +7.7)$ km s^{-1} for (U, V, W).

2.3. Orbit calculations for the halo stars

For the numerical integration of the orbits the Galactic mass model of Allen & Santillán (1991) was used. Although the model is quite simple, it represents well the observed data most directly related to the quantities that determine the Galactic orbits. The model consists of three components: a central spherical mass distribution and a disk, both of the Miyamoto-Nagai form, and a massive spherical halo. The resulting rotation curve is nearly flat from about 20 kpc out to 100 kpc, and agrees well with the observed values in the range 1 to 20 kpc. The model-predicted run with z of the perpendicular force, K_z, also agrees well with observational data. The Galactic parameters upon which the model is based are $R_\odot$ = 8.5 kpc, V_0 = 220 km s^{-1} and a total local mass density of $\rho = 0.15 M_\odot$ pc^{-3}. The resulting values for the Galactic constants are A = 12.95 km s^{-1} kpc^{-1} and $B = -12.93$ km s^{-1} kpc^{-1}, in good agreement with recent determinations. If the spherical halo reaches 100 kpc the total mass of the model Galaxy is about $9 \times 10^{11}\ M_\odot$. The model potential is fully analytical, continuous, and with continuous derivatives everywhere; the density can be obtained in closed form and is positive everywhere; the mathematical simplicity of the model allows rapid, accurate, and reproducible numerical orbit integrations.

The orbits were computed using a 7th order Runge-Kutta-Fehlberg integrator with automatic step-size control. The fractional error in the energy at the end of the runs was usually smaller than 10^{-6}; the error in h, the z-component of the angular momentum was about an order of magnitude smaller. Each orbit was integrated backwards in time for 1.6×10^{10} years or 1000 time steps, whichever occured first. This time was found to be sufficient to allow the classification of the orbit in most cases, but many orbits were run for significantly longer times, as explained below in Section 5.

There is now increasing evidence suggesting that the Milky Way is a barred spiral galaxy. (See for example chapter 2 of Blitz & Teuben, 1996). Such a non-axisymmetric contribution has not been considered in the Galactic model of Allen & Santillán, but its inclusion would only increase the importance of orbital chaos over that estimated here, due to the destruction of the isolating integrals of motion for stars crossing the Galactic plane within 2-3 kpc of the Galactic center (Binney & Tremaine 1987). However, a bar, as well as other perturbers such as molecular clouds, warps, and spiral arms, would tend to smear and to make more diffusive the chaotic structure discussed below in section 5.

2.4. Surfaces of section and meridional orbits; definitions and classification of orbits

In the following nomenclature "vertical" refers to a direction perpendicular to the Galactic plane and "horizontal", parallel to this plane.

To classify and to better visualize the halo-star orbits, horizontal surfaces of section (HS), a form of Poincaré section, have been plotted for all 280 halo stars. Examples of such HS are seen in Figs. 6 and 7 of Paper IV and in Figs. 2-9 below. These figures are constructed by plotting Π vs $\tilde{\omega}$, i.e. U vs $\tilde{\omega}$ (the radial Galactocentric velocity vs the radial Galactocentric position), each time the star crosses the Galactic plane, z = 0 kpc. These HS are symmetric about Π = 0 km s^{-1} due to the symmetry of the potential with respect to the Galactic plane.

The vertical surfaces of section (VS) proposed here, also a form of Poincaré section, are defined as a plot of Z vs z, i.e. W vs z (the Galactic vertical velocity vs vertical height), each time the orbit crosses the cylinder $\tilde{\omega}$ = 8.5 kpc with either an outward, $\Pi > 0$ km s^{-1}, or an inward, $\Pi < 0$ km s^{-1}, velocity. These VS are not symmetric about the Z = 0 km s^{-1} nor z = 0 kpc axes; the potential is not radially symmetric at $\tilde{\omega}$ = 8.5 kpc. But, the $\Pi > 0$ km s^{-1} VS and the $\Pi < 0$ km s^{-1} VS are mirror images of each other. Examples of VS are also seen in Figs. 2-9.

Meridional orbits are the same as defined in Paper IV and plotted there in Figs. 2-5 and here in Figs. 4-9; z is plotted versus $\tilde{\omega}$ while following the orbit around the Galaxy. They give a cross-sectional view of the orbit. The HS and meridional orbits have in the past been fairly typical tools in the analyses of stellar dynamics and Galactic orbits, such as in Hénon & Heiles (1964), Ollongren (1965), Paper IV, and Valera et al. (1994a). The VS that are proposed here allow a more complete understanding and visualization of the orbital structure of the halo stars, and a more direct comparison with observations. They provide useful information concerning the orbital structure perpendicular to the Galactic plane.

In general the three plots defined above have numerous uses, such as visualizing the orbits in phase space, classification of the orbits into categories such as chaotic, box, or resonant, a better understanding of the effects and structure of chaos, and comparison with radial-velocity observations. For example, the VS can be readily compared to radial-velocity observations and distributions at the Galactic Poles; a histogram of Z across such a VS corresponds to the radial-velocity distribution that would be observed at a Galactic Pole for an ensemble of orbits with a given energy, angular momentum, and initial conditions.

In this paper the discussions make use of specialized terms, such as "chaotic" and "quasiperiodic" orbits, "island chains", "KAM surfaces", "sticking" to KAM surfaces, and "intermittency transition to chaos". In general the standard definitions and nomenclature, such as presented in the works by Hénon & Heiles (1964), Ott (1993), and Karney (1983), are used. For example, a "KAM surface" refers to the mathematical work of Kolmogorov, Arnold, and Moser (KAM) concerning the perturbation of integrable Hamiltonian systems. A KAM surface refers to the outer island, or torus for higher dimensions, in phase space of integrable, i.e. non-chaotic, orbits. Such a torus survives a small perturbation if the orbit is quasiperiodic, but does not if it is periodic, or resonant, leading to an intricate maze of island chains around islands of other chains *ad infinitum* (Ott 1993). When a KAM surface begins to break up, the slightly broken, or perforated, tori are referred to as "cantori".

The scheme of orbital classification and the identification of chaos used here have been outlined in Figs. 2-7 of Paper IV and is based upon the work of Ollongren (1965) for an axisymmetric potential. It should be noted that this scheme is distinct from a more recent one used to classify orbits in non-axisymmetric potentials (Binney & Tremaine 1987). Here a "box" orbit ("b" classification) densely fills a box-like figure in the meridional plane and delineates simple one-dimensional curves in the HS and VS; see Figs. 2 and 6 of Paper IV. A resonant orbit by definition shows a resonance between its vertical and horizontal motions. The "tube" orbit ("t" classification) of the star G48-29 shown in Fig. 5 of Paper IV is that of a 1:1 resonance. See also Fig. 9. A comparison of the number of islands in the HS and VS frequently will give the degree of the resonance, such as 1:1 or 2:3. "Chaotic" orbits ("c" classification) generally show irregular meridional projections, and in the HS and VS fill two-dimensional surfaces which are confined to lie between the curves of the box and/or resonant orbits; see Fig. 3 of Paper IV and Figs. 2-8 below. Chaotic orbits have one less isolating integral of motion than do the b and t orbits (Hénon & Heiles 1964; Valera et al. 1994a). The box-box ("bb") orbit of G206-34 shown in Figs. 4 and 7 of Paper IV is essentially a chaotic orbit highly constrained between box and resonant orbits. Most of our orbital classifications have been quickly and clearly done using only the meridional orbits and the HS; occasionally a longer orbital integration was needed to obtain an unambiguous classification. Some orbits appear to be boxes ("b") or tubes ("t") but upon closer inspection show some small scatter indicative of incipient chaos; these have been given classifications, "bc" or "tc".

3. The z_{max} versus $|W'|$ correlation

Generally our results agree with those of Grenon (1987, 1989), Paper IV, and Valera et al. (1994a) concerning the prevalence of, and reasons for, chaos in the Galactic halo. From our total sample of 280 halo stars, 44.3% are found to have chaotic orbits, including such marginal cases as the bc and tc classifications. 45.1% of the halo stars from the SN catalogue and 41.9% from the SPC catalogue have chaotic orbits; this small difference probably stems from the stronger kinematic bias of the SN catalogue, leading to a larger number of nearly radial orbits. Valera et al. (1994a) integrated orbits for the same 280 halo stars, same initial conditions, and same Galactic potential of Allen & Santillán (1991). However they used a different computer and a program with only a fourth-order integrator. Many of the stars ($\sim$ 20%) had different orbital classifications than here, but the ensemble results were very similar. They found 41.1% to be chaotic orbits. Using the Galactic potential of Bahcall et al. (1982, 1983), 46.8% chaotic orbits were found, and with the potential of Caldwell & Ostriker (1983), 33.6%.

Also, for 133 b orbits $\langle|h|\rangle$ = 922.2 $\pm$ 513.3 kpc km s^{-1} and $\langle R_{min}\rangle$ = 2.96 $\pm$ 1.87 kpc, where h is the angular momentum of the orbit about the z-axis and corresponds to one of the isolating integrals of motion. For 20 t and tc orbits, $\langle|h|\rangle$ = 462.3 $\pm$ 223.6 kpc km s^{-1} and $\langle R_{min}\rangle$ = 1.31 $\pm$ 0.56 kpc,

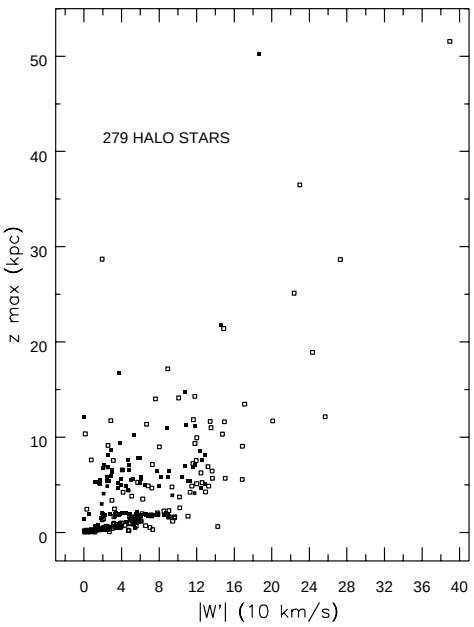

Fig. 1. The z_{max} values from the orbital integrations are plotted as a function of the observed $|W'|$. Stars with chaotic orbits are shown by filled squares while those with non-chaotic orbits by open squares

and for 111 c orbits, $\langle|h|\rangle$ = 219.7 $\pm$ 150.2 kpc km s^{-1} and $\langle R_{min}\rangle$ = 0.47 $\pm$ 0.36 kpc. Sixteen stars with higher-order resonant orbits or transitional orbits, such as the "bc"'s, have not been included in such averages. The above averages show that indeed the orbital angular momentum is crucial for producing chaos. Stars with low angular momenta penetrate the inner 1 kpc of the Galaxy where the spherical components, mainly the central bulge, dominate leading to the "scattering" of orbits which produces the chaotic behaviour. But, a purely spherical bulge would not produce chaos; it is the perturbation of the disk potential upon the dominating spherical component that produces the chaotic scattering in the central regions of the Galaxy.

In Fig. 1 is plotted the z_{max} vs $|W'|$ diagram for 279 of the halo stars; the star W7547, which has a t orbit and z_{max} = 77.7 kpc, has been excluded. In the figure stars with chaotic orbits are represented by solid squares and with non-chaotic orbits by open squares; z_{max} is the maximum distance above the Galactic plane reached in a star's orbit. It is seen that even for the non-chaotic orbits, there is not a well defined correlation between z_{max} and $|W'|$. For our 3-dimensional orbits, the vertical and horizontal movements are inter-related in a complicated way. Even for the box orbits, z_{max} is not obtained from $|W'|$ and from a simple integration of the vertical Galactic potential, as in a 1-dimensional case. In the 3-dimensional case, the observed $|W'|$ is only roughly indicative of the z_{max} for the most current vertical oscillation. The chaotic orbits increase the dispersion of Fig. 1 even more due to the "scattering" or mixing of the vertical and horizontal orbital energies. For the 46 c orbits with $z_{max} < 3.0$ kpc, $\sigma_{W'}$ = 56.7 km s^{-1}, and for 65 c orbits with $z_{max} > 3.5$ kpc, $\sigma_{W'}$ = 69.1 km s^{-1}; there is little difference in the $\sigma_{W'}$'s. For the b orbits on the other hand, 89 with $z_{max} < 3.0$ kpc have $\sigma_{W'}$ = 40.3 km s^{-1}, and 43 with $z_{max} > 3.5$ kpc have $\sigma_{W'}$ = 167.4 km s^{-1}, a considerable difference in the $\sigma_{W'}$'s.

These results agree well with those discussed in relation to Fig. 11 of Carney et al. (1990a). Even for the case with the restrictions, $|U| \leq 130$ km s^{-1}, $R_{apo} \leq 12$ kpc, and $R_{peri} \geq 1$ kpc, there is not a clean correlation between $|z_{max}|$ and $|W|$; these restrictions would tend to eliminate most of the chaotic orbits. For nearly their full sample, with only the restriction $R_{apo} \leq 40$ kpc, the correlation between $|z_{max}|$ and $|W|$ is very poor indeed. The stars with $|U| > 130$ km s^{-1} show a very large scatter; many of these penetrate the inner 1 kpc of the Galaxy.

One must conclude that the observed W' velocity is not a good parameter for studying chemical gradients in the Galaxy. Even for the more regular box orbits, W' measures only roughly the vertical excursion of the most recent vertical oscillation. And for the chaotic scattering, the vertical and horizontal orbital energies are mixed even more. So, in general W', does not give clean, unambiguous information about the original locations of stellar formation, especially not for the chaotic orbits. $z_{max,min}$ and R_{max} from the orbital integrations do generally give good estimates for the periodic and quasiperiodic box and resonant orbits, but for the chaotic orbits only upper limits to the possible vertical and radial excursions.

4. A chemical gradient in the Galactic halo?

With the above caveats in mind, Table 1 is presented with the purpose of detecting whether or not a chemical gradient is present in the Galactic halo. Regressions of [Fe/H] against R_{max} and z_{max} are given for the 280 halo stars and for various subsets. Nine halo stars have $R_{max} > 50$ kpc, lie somewhat apart from the bulk of the halo stars, and so tend to dominate, at times, the results; these nine stars have been removed from some of the regressions of Table 1; three of these have chaotic orbits and six non-chaotic. The last column of Table 1 shows the confidence level at which we can accept the hypothesis of a non-zero regression coefficient; a 50% confidence would indicate absolutely no evidence for a non-zero gradient.

Regressions have been carried out for the total halo sample, for those with non-chaotic orbits, and for those with chaotic, with and without the nine stars mentioned above. According to Table 1 there is very little evidence for a chemical gradient as a function of z_{max} in the Galactic halo. All confidence levels involving z_{max} are less than 87%, and the largest occurs for a positive regression coefficient, opposite what one might expect for the Galactic halo. The most significant regressions occur against R_{max} for the total sample (97.6%) and for the chaotic sample (99.4%), and with negative coefficients. However, most of this significance occurs due to a few outlying stars. Where one might expect to see the cleanest most unambiguous results, for the non-chaotic sample minus the outliers, the confidence levels are poor, 51.6% against R_{max} and 74.9% against z_{max}.

Table 1. Regressions of the photometric [Fe/H] values against the orbital parameters R_{max} and z_{max} for different subsets of the 280 halo stars. The last column shows the confidence at which the hypothesis of a non-zero metallicity gradient can be accepted

Group	Independent Variable	Regression Coefficient	Standard Error	Number of Stars	T-Ratio	Confidence Level (%)
Total	R_{max}	−0.00357	0.00180	280	1.983	97.6
Total	z_{max}	+0.00170	0.00172	280	0.992	83.4
Total–9	R_{max}	−0.00569	0.00469	271	1.214	88.3
Total–9	z_{max}	−0.00072	0.00701	271	0.103	54.1
Non-chaotic	R_{max}	+0.00088	0.00301	156	0.292	61.5
Non-chaotic	z_{max}	+0.00199	0.00174	156	1.144	86.7
Non-chaotic–6	R_{max}	+0.00021	0.00516	150	0.041	51.6
Non-chaotic–6	z_{max}	−0.00556	0.00812	150	0.685	74.9
Chaotic	R_{max}	−0.00530	0.00208	124	2.548	99.4
Chaotic	z_{max}	+0.00132	0.00850	124	0.155	56.2
Chaotic–3	R_{max}	−0.00966	0.01154	121	0.837	79.7
Chaotic–3	z_{max}	+0.00048	0.01278	121	0.037	51.5

One must conclude from Table 1 that there is not overwhelming evidence for a chemical gradient in the Galactic halo.

These results agree with those of Zinn (1985) concerning the outer-halo globular-cluster population of the Galaxy, and with the results of Carney et al. (1990a) and SPC, who make use of halo field stars from various high-velocity and proper-motion catalogues, but disagree with the conclusions of Sandage (1981) and Sandage & Fouts (1987) who find a "wedge- shaped" distribution in the W' versus $\delta(0.6)$ diagram.

Zinn (1985) found that the typical halo globular clusters, those with [Fe/H] < -0.8, in the outer–halo, $R \gtrsim R_{\odot}$, show no evidence for a chemical gradient, $\Delta[\mathrm{Fe/H}]/\Delta R$ = +0.004 ± 0.010 dex kpc^{-1}. Carney et al. (1990a) examine their halo sample in various $|W|$ vs $\delta(U-B)_{0.6}$, $|W|$ vs [m/H], [m/H] vs R_{apo}, and [m/H] vs $|z_{max}|$ diagrams and find no evidence for a chemical gradient; for example, $\Delta[\mathrm{m/H}]/\Delta R = -0.008 \pm 0.008$ and also $\Delta[\mathrm{m/H}]/\Delta|z_{max}| = -0.008 \pm 0.008$ for their most extreme halo sample, $V \leq -200$ km s^{-1} and $R_{apo} \leq 40$ kpc. SPC point out that the conflicting results of Sandage (1981) and Sandage & Fouts (1987) are mostly likely due to a significant contamination by the Galactic thick disk; these authors used only $|V'| > 100$ km s^{-1} to select their "halo" sample. Also, as discussed above, the W' velocity is not adequate for the study of chemical gradients in the Galactic halo.

5. Examples of interesting VS, HS, and meridional orbits

In this section a number of interesting VS, HS, and meridional orbits are given and discussed with the aim of showing what sort of phase-space structure may exist in the Galactic halo due to the interaction between chaotic orbits and families of quasiperiodic and/or resonant orbits. For the figures given in this section the orbital integrations have been carried out for much longer times than for the results of the other sections. For example, for the orbital parameters such as $z_{max,min}$ or $R_{max,min}$ the orbits were integrated for 1000 time steps or for 16 Gyr whichever came first. Here the VS and HS are plotted for integrations of as long as 25,000 time steps, and the meridional orbits for as long as 6000 time steps. These time intervals correspond to ages much longer than that of the Galaxy. These longer integrations are not meant to represent a single star but are given to better depict the phase-space structure of the orbits; they might better be thought of as representing an ensemble of stars with similar orbital energies, angular momenta, and initial conditions. In every case the phase-space structure investigated with these long orbital integrations was first detected with the shorter orbital integrations used for the orbital parameters.

Figs. 2-8 are given to exemplify two terms, "stickiness" and "confinement", which will be used to describe two physical processes related to chaotic Galactic orbits, which may be important for understanding the phase-space structure of the Galactic halo. "Stickiness" is a term used in the literature (for example, see Karney 1983; Meiss & Ott 1985; Ding et al. 1990; Hanson et al. 1985; Ott 1993; Kandrup & Mahon 1994) to describe the behaviour of chaotic orbits which pass near the outer limiting tori of a family of quasiperiodic and/or resonant orbits. The break-up of the last KAM torus leads to a very intricate region of island chains and cantori in phase space through which the chaotic orbit must diffuse. This impeded diffusion has a long-time power-law decay of particles (stars) from a given volumn of phase space rather than the exponential decay which is usually found for chaotic orbits (see, for example, Ding et al. 1990). This phenomenon has also been referred to as "anomalous diffusion" (Ishizak et al. 1991), "clustered motion" (Konishi & Kaneko 1994), "trapping" (Kandrup & Mahon 1994), and "leaky barriers" (MacKay et al. 1984a,b). Such structure within chaos can be

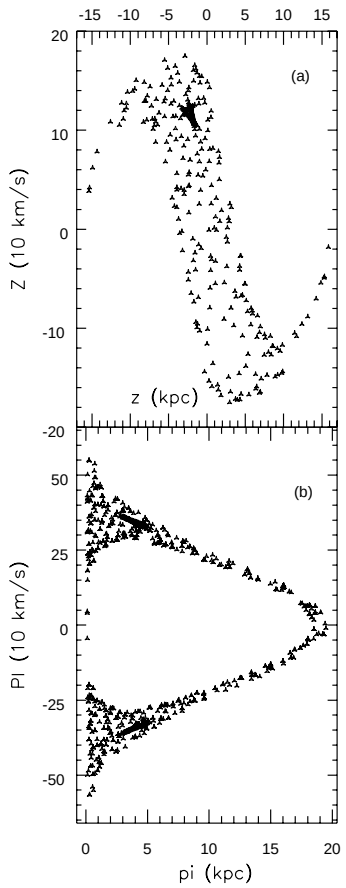

Fig. 2a and b. The vertical and horizontal surfaces of section for the halo star $-45°3283$, which has a chaotic orbit. These plots show clear evidence of the "sticking" phenomenon for chaotic orbits discussed in the text. **a** The vertical surface of section Z plotted versus z each time the orbit crosses the cylinder $\tilde{\omega}$ = 8.5 kpc with an outward velocity ($\Pi > 0$ km s^{-1}). **b** The horizontal surface of section, Π (PI) plotted versus $\tilde{\omega}$ (pi) each time the orbit crosses the Galactic plane, z = 0 kpc

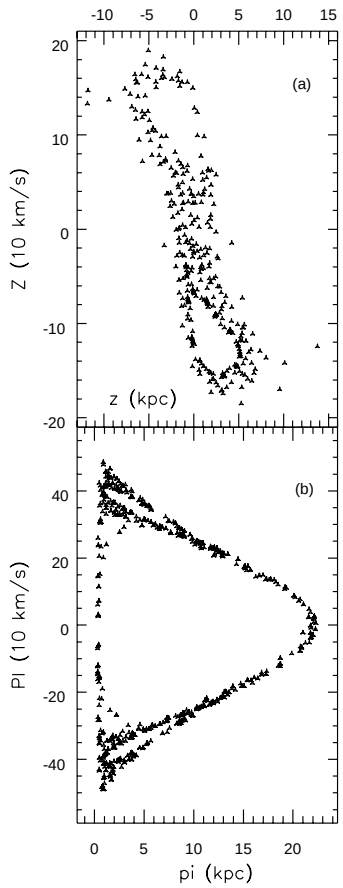

Fig. 3a and b. The same as Fig. 2 but for the halo star G192-043, which also has a chaotic orbit demonstrating the "sticking" phenomenon

especially appreciated in Fig. 6 of Hénon & Heiles (1964) and in Fig. 14 of Hénon (1969). It has generally been investigated for low-order dynamical systems, but Ding et al. (1990) show that such effects also occur for higher dimensional Hamiltonian systems (using four- and six-dimensional symplectic maps). Fig. 6 of Soper et al. (1990) shows that structure within chaos may also occur for asteroid orbits within the solar system and that its appearance in phase space is quite distinct from that produced by low numerical accuracy.

"Confinement" here refers to a process similar to that discussed by Wisdom (1987) for the orbital eccentricities of asteroids related to the formation of the 3/1 Kirkwood Gap, such as shown in the surface of section of his Fig. 9. For some initial conditions, the chaotic orbit is restricted ("confined") by families of quasiperiodic and/or resonant orbits to spend most of its time in a fairly well defined region of phase space but with narrow branches leading to much larger excursions. For asteroids these larger, irregularly occurring excursions are to larger orbital eccentricities producing planet-crossing trajectories, which after a long enough time sweep the gap clean of asteroids (see also Wisdom 1983). For the stars studied here the chaotic trajectories are "confined" by a major 1:1 resonant family in the Galaxy to spend most time within about 2 kpc of the Galactic plane; $|z_{max,min}| \lesssim 2.5$ kpc. However, narrow branches in phase space allow the chaotic orbits to occasionally and irregularly escape around the resonant family to higher altitudes; $|z_{max,min}| \approx 3$ to 7 kpc. Such a process may produce a non-primeval vertical duality in the Galactic halo.

Figs. 2 and 3 show the HS and VS for the chaotic halo stars $-45°$ 3283 and G192-043, which are clear examples of the "sticking" or "clustering" mentioned above. These orbits are clearly chaotic, filling two-dimensional areas in the surfaces of section, but also spend considerable time "stuck" near the interfaces of families of quasiperiodic orbits. The orbit of $-45°$ 3283 is also interesting in that it probably is a higher-dimensional example of an "intermittency transition to chaos" as discussed by Ott (1993). The time sequence cannot be appreciated in Fig. 2, but the orbit of $-45°$ 3283 starts out in the large chaotic region; then becomes "stuck" for a time in the interface region with the quasiperiodic orbits, appearing for awhile almost like a quasiperiodic orbit; and finally returns to the large chaotic region.

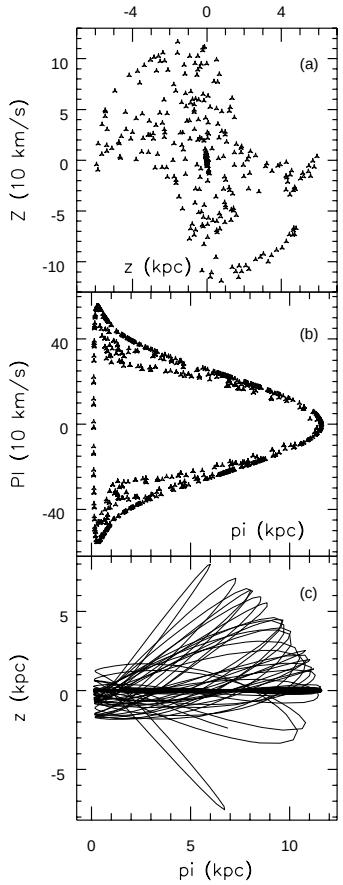

Fig. 4a–c. The vertical and horizontal surfaces of section and also the meridional orbit for the halo star G113-040, which has a chaotic orbit. **a** The vertical surface of section, as in Figs. 2 and 3, **b** The horizontal surface of section, as before, and **c** The meridional orbit, z is plotted versus $\tilde{\omega}$ while following the star around the Galaxy. This is an example of a chaotic orbit that gets "stuck" near the Galactic plane

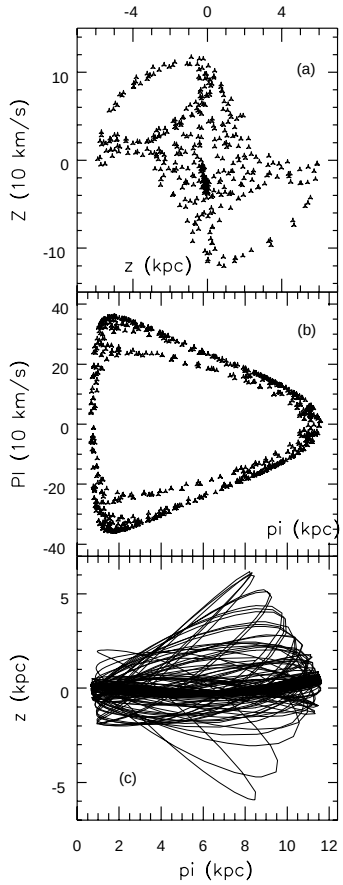

Fig. 5a–c. The same as Fig. 4 but for the halo star G217-008, which also has chaotic orbit that gets "stuck" at times near the Galactic plane

Figs. 4 and 5 show a slightly different aspect of this "sticking" to KAM surfaces; the HS, VS, and meridional orbits are shown for the chaotic halo stars G113-040 and G217-008. In the HS these two stars show occasional "sticking" to outer families of quasiperiodic orbits. During these episodes most of the stars' orbital energies are horizontal in the Galaxy, and so most of the orbital motion occurs near the Galactic plane, as clearly seen in the VS and in the meridional orbits. For intervals of time these stars are "stuck" near the Galactic plane.

In Figs. 6, 7, and 8 are shown good, clear examples of the "confinement" of orbits discussed above; the HS, VS, and meridional orbits are shown for the halo stars G159-050, HD74000, and G020-024. The VS of these stars show that they spend most of their time inside quadrangular areas of phase space, remaining within about $\pm$1.5 to 2.5 kpc of the Galactic plane, but each has narrow branches within the permitted region of phase space allowing occasional larger excursions to $\pm$ 3-7 kpc. The HS of these stars show multi-box-like structure similar to the "box-box" orbit of G206-34 shown in Fig. 7 of Paper IV. The meridional orbits demonstrate even more clearly that for most turns around the Galaxy these halo stars are confined thick-disk-like to within about $\pm$1.5 to 2.5 kpc of the Galactic plane but that infrequently excursions to higher altitudes, $|z_{max,min}| \approx 3$ to 7 kpc, occur.

Fig. 9 displays the HS, VS, and meridional orbit of the star G015-010 which has a tube-like, 1:1 resonant orbit. This star belongs to the family of periodic and quasiperiodic orbits which plays such an important role in defining the "stickiness" and "confinement" of the local halo stars with chaotic orbits, discussed above.

6. Vertical structure in the Galactic halo

The observed W' histogram for the sample of 280 halo stars is shown in Fig. 10. As discussed above, this velocity component has been constructed for each halo star using a photometric distance and radial velocities and proper motions from the literature. In Fig. 10 the upper curve shows the full set of 280 halo stars while the curve delineating the hatched region in the histogram corresponds to the halo stars with chaotic orbits according to our orbital calculations and classifications. The curves are clearly seen to be non-Gaussian. The upper curve contains two peaks, a principal one centered on the interval $-30 < W' \leq -10$ km s^{-1} and a secondary one on the inter-

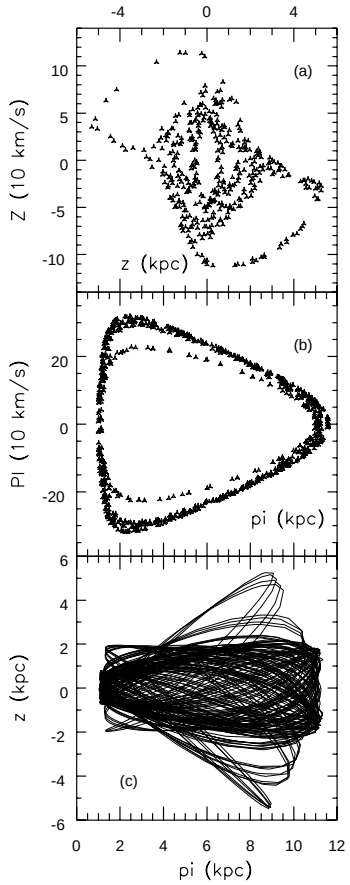

Fig. 6a–c. The same as Fig. 4 but for the halo star G159-050, which has a chaotic orbit with most of its orbital motion "confined" to within $\sim$ 2.5 kpc of the Galactic plane

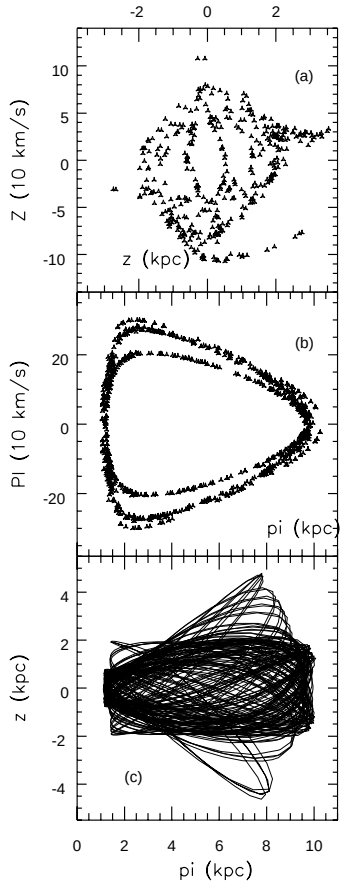

Fig. 7a–c. The same as Fig. 4 but for the chaotic halo star HD74000

val +50 $< W' \leq$ +70 km s^{-1} (marked by small arrows). It is seen in Fig. 10 that this secondary peak in the W' histogram is produced in large part by the halo stars with chaotic orbits.

In Fig. 11 is given the z_{max} histogram for the sample of 280 halo stars. Here, z_{max} is the maximum distance above the Galactic plane attained by a star in its orbit during an integration of 1000 time steps or 16 Gyr, as explained above. The histogram against z_{min}, the maximum distance below the Galactic plane, is very similar to that of Fig. 11. The upper curve is for the full sample of 280 halo stars while the lower demarcates the subset with chaotic orbits. Considerable structure is seen in these histograms. The upper curve shows a major peak in the Galactic plane for $z_{max} < 1.5$ kpc, a second important peak over the interval $1.5 < z_{max} \leq 2.0$ kpc, a minimum at $z_{max} \sim 3.0$ to 3.5 kpc, and a broad peak over $4.0 \lesssim z_{max} \lesssim 8.0$ kpc. It can be clearly seen that much of this structure, especially the peaks over $1.5 < z_{max} \leq 2.0$ kpc and $4.0 \lesssim z_{max} \lesssim 8.0$ kpc, is produced by the chaotic orbits.

As discussed above, the overall percentage of chaotic orbits is 44.3% for the total sample of 280 halo stars, while in Fig. 10 the peak over the interval +50 $< W' \leq$ 70 km s^{-1} with 26 stars includes 69.2% chaotic orbits (18 stars), and in Fig. 11 the peak over $1.5 < z_{max} \leq 2.0$ kpc with 45 stars, 66.7% chaotic orbits (30 stars). In addition, of the 26 stars in the +50 $< W' \leq$ +70 km s^{-1} peak of Fig. 10, 46.1% (12 stars) are also in the $1.5 < z_{max} \leq 2.0$ kpc peak of Fig. 11, while for comparison the overall percentage of inclusion is only 16.1%, and for the peak at $-30 < W' \leq -10$ km s^{-1} of Fig. 10, only 19.4% (6 stars) fall also in the $1.5 < z_{max} \leq 2.0$ kpc peak of Fig. 11; a rather amazing correlation between the structure of Fig. 10, which is a histogram based on observed data, and the structure of Fig. 11, which is the result of orbital integrations. This correlation is produced largely by the halo stars with chaotic orbits in spite of the fact that the correlation between z_{max} and W' is very poor for chaotic orbits, as discussed previously. And finally, of the 20 stars with tube orbits (1:1 resonances, "t" or "tc" classifications) 85% have either z_{max} or z_{min} in the interval 1.5-2.0 kpc; if the interval is redefined to 1.32-1.91 kpc, then 95% (19 out of 20) have z_{max} or z_{min} in the interval. So, the observed W' histogram and the calculated $z_{max,min}$ histogram both show structure, and this structure is correlated and is produced in large part by the chaotic and by the 1:1 resonant orbits.

To explain the structure and correlation of Figs. 10 and 11, the "confinement" of chaotic orbits by a family of quasiperiodic orbits, as discussed above, plus Figs. 6-8 are employed. The VS and meridional orbits of the stars G159-050, HD74000,

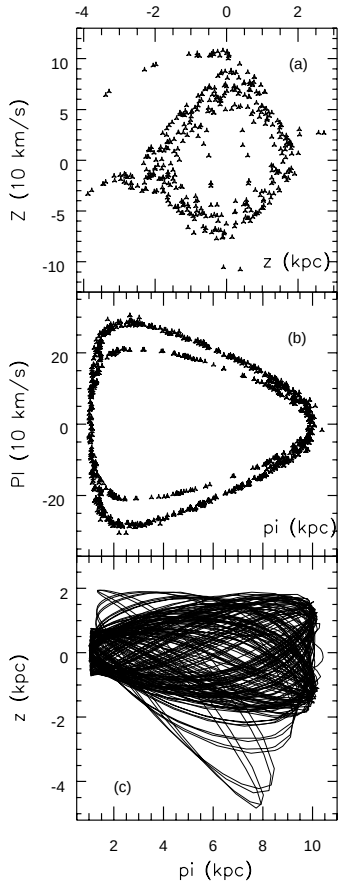

Fig. 8a–c. The same as Fig. 4 but for the chaotic halo star G020-024

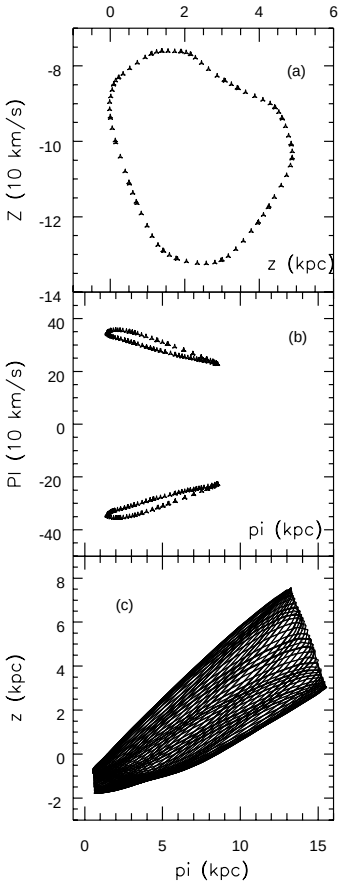

Fig. 9a–c. The same as Fig. 4 but for the tube orbit of the halo star G015-010.

and G020-024 show that they are confined to within 1.5 to 2.5 kpc of the Galactic plane for most of their orbital motions, escaping to higher altitudes only occasionally through narrow branches in phase space. These narrow branches lie around a family of quasiperiodic orbits which is situated $\sim$ 1-4 kpc above the Galactic plane at the solar distance from the Galactic center. So, in Fig. 11 the $z_{max} \sim$ 1.5-2.0 kpc peak corresponds to the edge of the quadrangular areas in phase space where stars like G159-050, HD74000, and G020-024 spend most of their orbital motion. Chaotic halo stars which have already escaped through the narrow branch in phase space are found in the $z_{max} \sim$ 4.0-8.0 kpc peak of Fig. 11, and the minimum over $z_{max} \sim$ 3.0-3.5 kpc corresponds to that part of the quasiperiodic family of orbits which extends above 2.5 kpc. The tube orbits found in the peak at $z_{max} \sim$ 1.5-2.0 kpc belong to this family of quasiperiodic orbits, lying in the outer (lower) fringes of the family and so are able to pass through the solar vicinity.

Numerical experiments generally confirm this interpretation of Fig. 11. For $z_{max} > 3.5$ kpc, 59.1% of the orbits are chaotic, and for $z_{max} < 3.0$ kpc, 34.4%. If the orbital integrations of the 280 halo stars are extended beyond 1000 time steps or 16 Gyr, the peak over $z_{max} \sim$ 1.5-2.0 kpc **slowly** disappears, the peak over $z_{max} \sim$ 4.0-8.0 kpc increases in strength, and the percentage of chaotic orbits in the upper halo ($z_{max} > 3.5$ kpc) increases at the expense of the percentage in the lower halo. For the longer orbital integrations more and more of the chaotic orbits have an opportunity to escape to higher z_{max}'s through the narrow branches in phase space.

7. Discussion

7.1. Duality of the Galactic halo

In recent studies, such as those of Hartwick (1987), Norris (1993), and Kinman et al. (1994), evidence has been found pointing toward a duality in the Galactic halo. Hartwick (1987) used the more metal-poor RR Lyrae stars for his work and found indications in their spatial distribution for a two-component halo with a flattened inner component, c/a $\sim$ 0.6 and scale height $\sim$ 1.7 kpc, and a nearly spherical outer one. The metallicity distributions of the two components were very similar, ruling out a dissipative collapse with chemical evolution for the formation of the flattened inner component; and Hartwick (1987) concluded, "... the dominant flattening mechanism is due to the dynamical evolution of an extant population of stars ...".

Kinman et al (1994) studied blue horizontal branch stars outside the solar circle finding for $z > 5$ kpc evidence for a classical spherical halo, while closer to the Galactic plane evi-

dence for on additional, much flatter population of stars. The two components do not have significantly different metallicity distributions, but the flatter component does seem to be somewhat bluer indicating perhaps a somewhat larger age. Kinman et al. (1994) conclude, "... this analysis supports a two-component model for the halo of our Galaxy that is similar in many respects to that proposed by Hartwick ..."

Also, recently Norris (1993) has used a dual-halo model, with "accreted" plus "contracted" components, to explain the correlation of the W'–velocity dispersion with [Fe/H] for the survey stars of Carney et al. (1990a). The "accreted" component is analogous to the stars that would form during an infall of "protogalactic fragments" model, such as that of Searle & Zinn (1978; SZ), and the "contracted" component to those of a radial, rapid collapse of a single protogalactic unit model, such as that of Eggen, Lynden-Bell, and Sandage (1962; ELS).

In the present work there are also several indications for structure and a possible dichotomy of the Galactic halo. In Fig. 11 a separation between a lower halo, $z_{max} < 3.0$ kpc, and an upper halo, $z_{max} > 3.5$ kpc. is clearly noted. As discussed above this dichotomy may be in part the result of dynamical evolution produced in the $z_{max,min}$ histograms by the interaction and confinement of the orbits of local stars, especially those with chaotic orbits, by a dominant 1:1 resonant family of orbits lying a few kpc above the Galactic plane at the solar distance from the Galactic center. Only more detailed observations and counts of halo stars and more extensive numerical simulations can show whether such a confinement and interaction process can produce the sort of distributions observed by Hartwick (1987), Norris (1993), and Kinman et al. (1994).

In addition to the vertical structure of Fig. 11, the present results also indicate a rather significant division of the halo stars into chaotic and non-chaotic kinematic groups. Table 2 summarizes several kinematic and orbital parameters for the different orbital classifications and vertical divisions. Only 264 halo stars are considered in Table 2; 16 halo stars with higher-order resonant orbits or transitional orbits, such as the "bc"'s have not been included. In the first half of Table 2 the halo stars have been divided into three groups according to their orbital classifications: 133 halo stars with box orbits ("b" classifications only), 111 halo stars with chaotic orbits ("c" classifications only), and 20 halo stars with "tube" 1:1 resonant orbits ("t" and "tc" classifications); the latter group contains seven of the "tc" transitional orbits and yet the overall group remains small, only 20 stars. The second half of Table 2 gives kinematic and orbital data for the upper, $z_{max} > 3.5$ kpc, and lower, $z_{max} < 3.0$ kpc, groups of Fig. 11.

Table 2 emphasizes several of the arguments made above: that the chaotic orbits are low-angular-momenta, plunging, highly eccentric orbits that penetrate the inner 1 kpc of the Galaxy, while the box orbits are higher-angular-momenta, more circular orbits that remain outside the inner 1 kpc; that for the chaotic orbits there is a very poor correlation between z_{max} and W'; and that in most aspects the 1:1 resonant orbits are more similar to the chaotic orbits than to the box orbits.

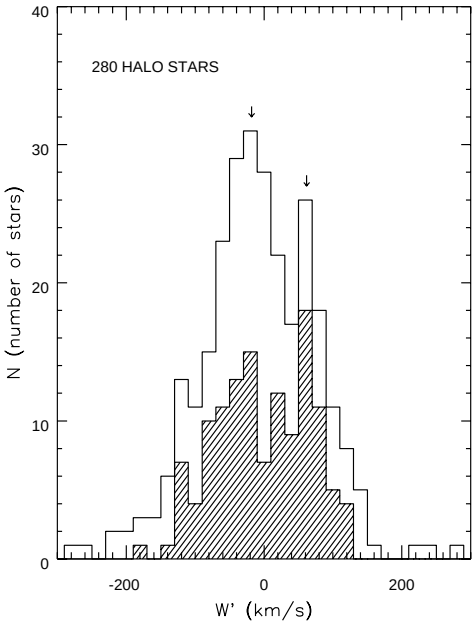

Fig. 10. The W' histogram for the 280 halo stars of this study. The upper envelope is for the total sample of 280 stars, while the hatched region shows the subset of halo stars with chaotic orbits. The small arrows mark the two peaks, +50 $< W' \leq$ +70 km s^{-1} and $-30 < W' \leq -10$ km s^{-1}, which are discussed in greater detail in the text

Table 2 also points out a couple of additional items: that, like the results of Hartwick (1987) and Kinman et al (1994), the [Fe/H] distributions of the upper and lower halo are very similar; and that, as discussed in SPC and in Majewski (1992), the box orbits show evidence for a vertical gradient in angular momentum with the upper halo, $z_{max} > 3.5$ kpc, showing a negative average angular momentum; the chaotic orbits show no such gradient, but one would expect chaotic orbits to be much more highly mixed vertically while the z–component of the angular momentum is unchanged by the chaotic "scattering" at the center of the Galaxy.

The chaotic processes mentioned above, such as the chaotic "scattering" and "confinement" of chaotic orbits by families of quasiperiodic orbits, cannot produce the sort of results obtained by Beers & Sommer-Larsen (1995): that a thick-disk-like component exists in the Galaxy to metallicities at least as low as [Fe/H] = -2.0. Such results were obtained in large part by studying V_{rot} vs [Fe/H] diagrams, and the the z–component of the orbital angular momentum (similar to V_{rot} for the solar vicinity) is an isolating integral of motion even for the chaotic orbits.

7.2. Clumping in velocity space

Various works in the literature, such as those of Eggen (1987), Poveda et al. (1992), Sommer-Larsen & Christensen (1987), Doinidis & Beers (1989), Croswell et al. (1991), Arnold & Gilmore (1992), Majewski (1992), and Majewski et al. (1994),

Table 2. Velocity dispersions, average orbital parameters, and average [Fe/H] values for different orbital classifications and different heights (z_{max}) in the Galaxy

Orbital group	$\sigma_{u'}$	$\sigma_{v'}$ (km s^{-1})	$\sigma_{w'}$	$(\sigma_{v'}/\sigma_{u'})^2$	$\langle ecc \rangle$	$\langle \lvert h \rvert \rangle$ (kpc km s^{-1})	$\langle R_{min} \rangle$ (kpc)	$\langle z_{max} \rangle$ (kpc)	N
box, "b" only	157.0	123.8	100.7	0.622	0.658 ± 0.188	922 ± 513	2.96 ± 1.87	4.18 ± 7.48	133
tube, "t" and "tc"	289.7	54.2	96.3	0.035	0.888 ± 0.083	462 ± 224	1.31 ± 0.56	9.88 ± 16.63	20
chaotic, "c" only	159.5	31.4	64.4	0.039	0.920 ± 0.067	220 ± 150	0.47 ± 0.36	4.72 ± 3.54	111

Group	$\langle h \rangle$ (10 kpc km s^{-1})	$\sigma_{w'}$ (km s^{-1})	$\langle$[Fe/H]$\rangle$ (dex)	N
$z_{max} < 3.0$ kpc, chaotic	$+1.55 \pm 33.55$	56.7	-1.39 ± 0.48	46
, box	$+25.69 \pm 93.27$	40.3	-1.67 ± 0.49	89
$z_{max} > 3.5$ kpc, chaotic	$+3.83 \pm 20.45$	69.1	-1.37 ± 0.52	65
, box	-21.90 ± 121.96	167.4	-1.68 ± 0.54	43

have suggested the existence of "moving groups" of stars in the halo and thick-disk of the Galaxy. Frequently these groups are seen as "clumps" in various velocity, metallicity, and/or spatial-distribution diagrams, such as the Bottlinger diagram or the [Fe/H] vs h diagram. Frequently it is argued that these moving groups are the remains of globular clusters that have been dissipated fairly recently during the history of the Galaxy. But, if such were the case, we would expect to find at least some moving groups in the halo with a considerable number of members; in fact, the recognized halo moving groups have at most a few dozen members. Furthermore, quite a number of such moving groups have been detected by various investigators, and it is difficult to understand, using time-scale arguments and considering the various dissipative processes of the Galaxy, how so many such recognizable dissipated globular clusters could be in existence at the present epoch.

The ages, metallicities and kinematics of the best known moving groups – like the Hyades and Sirius groups – clearly indicate that they belong to the disk population of the Galaxy. However, there are several groups known to belong to the thick disk or even halo populations. Such are the groups associated to Kapteyn's star and to Groombridge 1830. These old groups pose an interesting dynamical problem. Traditionally moving groups were interpreted to be clusters or associations already dissociated or on the verge of becoming so. Their member stars are in general unbound, but they still move with similar velocities and can be recognized by a careful analysis of their velocity vectors. As the group becomes older, after several revolutions about the Galactic center, a subset of its member stars will be spread along the orbit in a large arc, but will still be recognizable by the similarity of their V velocities. When the group becomes still older, after many more revolutions around the Galaxy, it merges into the general field and becomes unrecognizable. In this general picture, the existence of very old groups, like Kapteyn's and Groombridge 1830's, which have had time to perform a great many revolutions around the Galaxy, is very difficult to understand. They may be the remains of objects that were originally very populous (globular clusters or dwarf galaxies), they may be the remains of past mergers in the Galactic halo, "ghostly streams", or their coherence may be due to the confining effect of interacting periodic orbits in the Galactic potential, as is proposed here.

In addition, in several studies unusual, non-Gaussian velocity clumping has been detected at the Galactic Poles. A good example of this is found in Fig. 13(b) of Beers et al. (1985). Norris (1986) refers to the "... small-scale clumping in velocity space..." and Beers & Sommer-Larsen (1995), "... the non-Gaussian nature of the velocity distribution of extremely metal-poor stars ([Fe/H] ≤ -1.5) in the directions of the Galactic poles". The reader is also referred once again to the non-Gaussian appearance of Fig. 10; the great majority of these 280 halo stars are located within 300 pc of the Sun.

It is proposed here that the processes discussed above: the quasiperiodic orbits of the dominant 1:1 resonance lying 1-4 kpc above the Sun in the Galaxy, the confinement of chaotic orbits by this resonant family, and especially the sticking of the chaotic orbits to the outer fringes (in phase space) of this family, produce or help to maintain the observed clumping in phase space. For example, Figs. 2 and 3 above show such velocity clumping when a chaotic orbit, in a rather extended chaotic sea in phase space, penetrates the transition region between chaos and the quasiperiodic orbits; the chaotic orbit becomes "stuck" in the transition region, and its escape is governed by a rather lengthy power law, as discussed above in Sect. 5 and in references such as Karney (1983) and Ding et al. (1990). Figs. 4 and 5 above also show such clumping, at low velocities and near the Galactic plane, when the "sticking" is to outer quasiperiodic orbits with most of their orbital energy in the horizontal sense.

According to this proposal some halo moving groups may actually be created as a number of halo stars with chaotic orbits become "stuck" in the transitional border of the 1:1 resonant family, or, at least, these sticking and confinement processes al-

low the remains of dissipated globular clusters to be recognized as such for much longer time intervals than might otherwise be expected. A check of the HS and VS of the 124 halo stars which show chaos in their Galactic orbits indicates that about 73% (90 stars) demonstrate some evidence for the structure related to the "sticking" or "confinement" of chaotic orbits, that is, 32.5% = 90/280 of the total halo sample. This is probably a lower limit to the total number that will eventually exhibit such phenomena since the orbits were integrated only 1000 time-steps or 16 Gyr, whichever came first, and the "sticking" phenomenon tends to appear more and more the longer the orbits are integrated, e.g. the intermittency transition to chaos, and so forth. Of the 280 halo stars in our sample, 43.2% (121/280) have $R_{min} < 1.0$ kpc, though not all these (only 106 of 121) show evidence of chaos in their orbital structure. It is seen that such processes may involve something on the order of a third of the halo field stars.

Searle & Zinn (1978) propose that much of the Galactic Halo, especially the outer part, was formed by the coalescence and infall of protogalactic fragments. Preston et al. (1994) have detected blue, metal-poor main sequence stars and argue that these are evidence for accretion events by the Galaxy during the last 3 to 10 Gyr. Ibata et al. (1994) have discovered such an event in process: a dwarf galaxy with perhaps as many as four associated globular clusters is now undergoing tidal disruption and merger with the Galaxy in the direction of Sagittarius. So it is clear that some of the "velocity clumping" and "moving groups" are due to such occurrences, as well as due to the remains of disassociated Galactic globular clusters, but the fairly large number of sparse groups reported in the literature, with few or no intermediate sized groups, indicates that the chaotic structure discussed above is important for producing at least part of the phase-space clumping that has been detected.

7.3. Astronomical implications of orbital chaos

The following are possible ramifications of orbital chaos within the Galaxy:

As seen in Fig. 11 orbital chaos may produce a non-primordial dichotomy in the Galactic halo. In Paper VII it was argued that a primeval **radial** duality exists in the halo due to different dominating processes of formation, that the inner halo was formed mostly by an ELS-like radial rapid collapse of a single protogalactic unit while the outer halo more by a lengthy SZ-like accretion process involving several protogalactic fragments. So probably part of the structure of Fig. 11 is primeval and due to the origins of the Galaxy but part may be posterior to formation, due to other causes, such as the "confinement" of chaotic orbits, as discussed above, due to our manner of defining z_{max}, and due also to our sampling volume near the Galactic plane. The "confinement" and "sticking" of chaotic orbits may tend to emphasize the (flattened inner) halo in the solar neighborhood, and the results of Hartwick (1987), Norris (1993), and Kinman et al. (1994), for example, concerning a dual halo, may be due in part to such processes. Differing shapes and velocity dispersions obtained for the Galactic halo may depend on the extent to which a stellar sample has been affected by such phase–space structure.

Stars that might not otherwise be seen in the solar vicinity are found nearby due to the chaotic "scattering" near the Galactic center. This scattering causes irregular and large exchanges of vertical and horizontal orbital energies while the total energy is conserved. So, for example, a star formed high in the halo on a plunging orbit might later be scattered on a more horizontal orbit along the Galactic disk and through the solar vicinity. Halo stars formed high but with more circular orbits would not pass so near the Galactic center, would not be scattered, and so might never be found in the solar neighborhood.

Information concerning the location of star formation is lost due to the orbital chaos. Such a process produces considerable noise upon relationships involving orbital parameters such as z_{max}, z_{min}, or R_{max}, and so attempts to detect physical correlations in the Galactic halo, such as a chemical gradient, will be more difficult, or impossible. This combined with the preferential destruction of center–passing globular clusters may make it even more difficult to infer detailed location-of-formation for the ELS-like radial-collapse component of the halo. The stars and clusters of the outer halo were perhaps formed more during a SZ-like accretion process, have on the average more circular orbits, and so retain more orbital information concerning their origins.

As discussed above, stars with chaotic orbits may be "confined" or "stuck" in phase space to the outer KAM surfaces of quasiperiodic orbits and thereby maintain longer than expected, or even produce non-coeval, "moving groups" within the Galactic halo. That is, the remains of dissipated globular clusters remain recognizable in phase space longer than one might estimate due to such processes and/or halo stars with largely unrelated formation scenarios can be brought together in phase space to mimic a cluster remnant.

8. Conclusions

The following are the principal conclusions of this work:

1. The W' velocity is not a good measure for estimating z_{max} , the maximum distance above the Galactic plane obtained by a star in its orbit, especially for chaotic orbits. Chaos produces nearly random, large exchanges between horizontal and vertical orbital energies. Even for box orbits W' gives a reasonable, fairly accurate estimate of z_{max} only for the most recent orbital oscillation.
2. There is no good evidence for a chemical gradient in the Galactic halo, even when the stars with chaotic orbits are removed from the sample. The best correlation, [Fe/H] vs R_{max} (99.4% confidence), occurs mainly due to the effect of three outlying stars with chaotic orbits. This result agrees with those of Carney et al. (1990a) and of Zinn (1985) concerning the lack of a chemical gradient.
3. Chaotic "scattering" of Galactic orbits by the central 1 kpc of our Galaxy can act to destroy our knowledge of the location of halo-star formation, to hide correlations involving

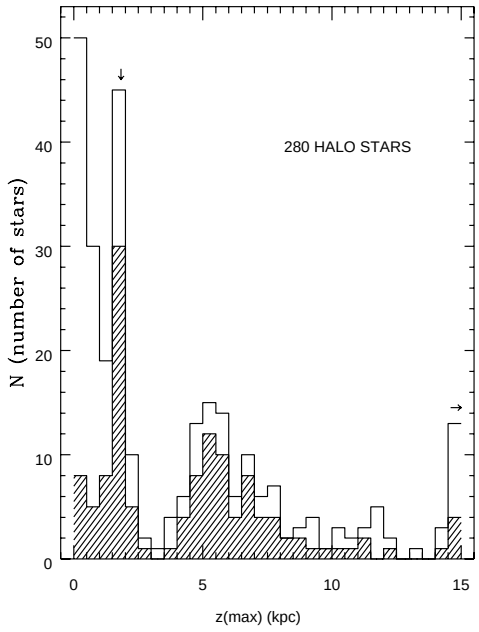

Fig. 11. The z_{max} histogram for the 280 halo stars. The upper envelope is for the total sample, while the lower hatched region shows the subset with chaotic orbits. z_{max} is the maximum distance above the Galactic plane attained by a star in its orbit during an integration of 1000 time steps or 16 Gyr. The small arrow marks the peak over the interval $1.5 < z_{max} \leq 2.0$ kpc, which is discussed in greater detail in the text

kinematic or orbital parameters, and to scatter into the solar neighborhood halo stars that might not otherwise be seen.

4. The vertical surfaces of section, as defined in Sect. 2.4, provide a good means for studying the phase-space structure produced by chaos, for analyzing the vertical structure of the Galactic halo, and for understanding the radial-velocity distributions observed at the Galactic Poles. Unlike the horizonal surfaces of section and the meridional orbits, these vertical surfaces of section have not found wide-spread previous use in the literature.
5. The $|W'|$ histogram for our sample of 280 halo stars and also various vertical surfaces of section for individual halo stars all show evidence for non-Gaussian velocity structure. Some of this structure in the observational $|W'|$ histogram seems to be correlated with that in the calculated z_{max} histogram, especially for the chaotic orbits, in spite of of the fact that the correlation between z_{max} and $|W'|$ is generally very poor for chaotic orbits, as discussed above. Also a very high percentage of the stars with 1:1 resonance tube orbits are found to lie in the 1.5-2.0 kpc peak of the z_{max} histogram. This structure and correlation is taken as evidence for the "confinement" and "sticking" of chaotic Galactic orbits by the outer KAM surfaces of families of quasiperiodic orbits, especially by a dominant 1:1 resonant family lying a few kpc above the Sun.
6. The "confinement" of the Galactic chaotic orbits is similar to that which Wisdom (1987) has discussed for the eccentricities of solar-system asteroids. In the Galactic case, the chaotic orbits are confined most of the time to within 1.5-2.5 kpc of the Galactic plane, but narrow branches exist in phase space that allow occasional escapes to altitudes of 4-8 kpc, contributing to a vertical duality in the Galactic halo. Such a process may serve to maintain and emphasize an "inner" halo in the solar vicinity, to produce in part the dual-halo results of Hartwick (1987), Norris (1993), and Kinman et al. (1994), and to explain the differing shapes and velocity dispersions obtained for the Galactic halo in the literature from stellar samples with different distance and selection criteria.
7. The "sticking" of chaotic orbits in the transition region beyond the last KAM surface of a family of quasiperiodic orbits has been discussed extensively in the literature, usually for lower dimensional dynamic systems, for sample by Karney (1983), Hanson et al. (1985), Meiss & Ott (1985), and Ishizaki et al. (1991). Ding et al. (1990) show that such a process is also important for higher-dimensional Hamiltonian systems. It is proposed here that this "sticking" in phase space may serve to explain the non-Gaussian ". . . clumping in velocity space. . . " (Norris, 1986) that has been observed for metal-poor stars near the Galactic Poles, and to maintain for longer intervals of time and/or to produce non-coeval "moving groups" within the Galactic halo.
8. In general it has been found here that the kinematics of Galactic halo stars are more complicated, intricate, and interesting than normally thought. Much work remains to be done via stellar surveys and observations of larger samples of halo stars and also via extensive numerical simulations to test the various conjectures set forth in this paper.

Acknowledgements. We especially wish to thank A. Santillán for carrying out many of the orbital integrations analyzed in this paper, F. Valera for some of the numerical tests, B. Hernández for computational assistance and Juanita Orta for helping to prepare the final manuscript. This work was partially supported by grants form CONACyT, Nos. D111-903865 and 1219-E9203, and DGAPA project No. IN101495. W.J.S. was visiting the Dept. de Astronomía, Instituto de Física, Univ. de Guanajuato, and the Institute of Physics and Astronomy, University of Aarhus, Denmark, when the final version of this paper was prepared; their hospitality was very much appreciated. We are also grateful to the referee, D. Pfenniger, for several useful suggestions.

References

Allen C., Martos M.A. 1986, Rev.Mex.Astron.Astrofís. 13, 137
Allen C., Santillán A. 1991, Rev.Mex.Astron.Astrofís. 22, 255
Allen C., Schuster W.J., Poveda A. 1991, A&A 244, 280 (Paper IV)
Arnold R., Gilmore G. 1992, MNRAS 257, 225
Bahcall J.N., Schmidt M., Soneira R.M. 1982, ApJ 258, L23
Bahcall J.N., Schmidt M., Soneira R.M. 1983, ApJ 265, 730
Beers T.C., Preston G.W., Shectman S.A. 1985, AJ 90, 2089
Beers T.C., Sommer-Larsen J. 1995, ApJS 96, 175
Binney J., Tremaine S. 1987, Galactic Dynamics. Princeton University Press
Blitz L., Teuben P. 1996, IAU Symp. 169, Unsolved Problems of the Milky Way. Kluwer Academic Publishers, Dordrecht
Caldwell J., Ostriker J.P. 1983, in Kinematics, Dynamics, and Structure of the Milky Way, ed. W.L.H. Shuter. Reidel, Dordrecht

Carney B.W., Latham D.W. 1987, AJ 93, 116
Carney B.W., Aguilar L., Latham D.W., Laird J.B. 1990a, AJ 99, 201
Carney B.W., Latham D.W., Laird J.B. 1990b, AJ 99, 572
Croswell K., Latham D.W., Carney B.W., Schuster W., Aguilar L. 1991, AJ 101, 2078
Ding M., Bountis T., Ott E. 1990, Phys. Lett. A. 151, 395
Doinidis S.P., Beers T.C. 1989, ApJ 340, L57
Eggen O.J. 1987, in The Galaxy, eds. G. Gilmore and B. Carswell. Reidel, Dordrecht, 211
Eggen O.J., Lynden-Bell D., Sandage A.R. 1962, ApJ 136, 748 (ELS)
Franklin F.A. 1994, AJ 107, 1890
Franklin F., Lecar M., Murison M. 1993, AJ 105, 2336
Froeschlé C., Scholl H. 1979, A&A 72, 246
Froeschlé C., Scholl H. 1981, A&A 93, 62
Grenon M. 1987, ESO Workshop Proceedings No. 27, 123
Grenon M. 1989, Ap&SS 156, 29
Gurzadyan V.G., Pfenniger D. 1994, Ergodic Concepts in Stellar Dynamics. Springer-Verlag, Berlin
Hanson J.D., Cary J.R., Meiss J.D. 1985, Journ. Stat. Phys. 39, 327
Hartwick F.D.A. 1987, in The Galaxy, eds. G. Gilmore and B. Carswell. Reidel, Dordrecht, 281
Hénon M., Heiles C. 1964, AJ 69, 73
Hénon M. 1969, Quart. Applied Math. 27, 291
Ibata R.A., Gilmore G., Irwin M.J. 1994, Nature 370, 194
Ishizaki R., Horita T., Kobayashi T., Mori H. 1991, Prog. Theor. Phys. 85, 1013
Johnson D.R.H., Soderblom D.R. 1987, AJ 93, 864
Kandrup H.E., Mahon M.E. 1994, A&A 290, 762
Karney C.F.F. 1983, Physica 8D, 360
Kinman T.D., Suntzeff N.B., Kraft R.P. 1994, AJ 108, 1722
Konishi T., Kaneko K. 1994, in Ergodic Concepts in Stellar Dynamics, eds. V.G. Gurzadyan and D. Pfenniger. Springer-Verlag, Berlin, 95
Laskar J. 1989, Nat 338, 237
Mackay R.S., Meiss J.D., Percival I.C. 1984a, Physica 13D, 55
Mackay R.S., Meiss J.D., Percival I.C. 1984b, Phys. Rev. Lett. 52, 697
Majewski S.R. 1992, ApJS 78, 87
Majewski S.R., Munn J.A., Hawley S.L. 1994, ApJ 427, L37
Marquez A., Schuster W.J. 1994, A&AS 108, 341 (Paper VII)
Meiss J.D., Ott E. 1985, Phys. Rev. Lett. 55, 2741
Nissen P.E., Schuster W.J. 1991, A&A 251, 457 (Paper V)
Nissen P.E., Twarog B.A., Crawford D.L. 1987, AJ 93, 634
Norris J. 1986, ApJS 61, 667
Norris J. 1993, preprint
Norris J., Bessel M.S., Pickles A.J. 1985, ApJS 58, 463
Ollongren A. 1965, in Galactic Structure, eds. A. Blaauw and M. Schmidt. Univ. Chicago Press, Chicago, 501
Ott E. 1993, Chaos in Dynamical Systems. Cambridge University Press
Petit J.M., Hénon M. 1986, Icarus 60, 536
Poveda A., Allen C., Schuster W. 1992, in IAU Symp. 149, The Stellar Populations of Galaxies, eds. B. Barbuy and A. Renzini. Kluwer, Dordrecht, 471
Preston G.W., Beers T.C., Shectman S.A. 1994, AJ 108, 538
Sandage A. 1981, AJ 86, 1643
Sandage A., Fouts G. 1987, AJ 93, 74
Schuster W.J., Nissen P.E. 1988, A&AS 73, 225 (Paper I)
Schuster W.J., Nissen P.E. 1989a, A&A 221, 65 (Paper II)
Schuster W.J., Nissen P.E. 1989b, A&A 222, 69 (Paper III)
Schuster W.J., Parrao L., Contreras Martínez M.E. 1993, A&AS 97, 951 (SPC)
Searle L., Zinn R. 1978, ApJ 225, 357 (SZ)
Sommer-Larsen J., Christensen P.R. 1987, MNRAS 225, 499
Soper P., Franklin F., Lecar M. 1990, Icarus 87, 265
Valera F., Schuster W., Aguilar L. 1994a, in Numerical Simulations in Astrophysics, eds. J. Franco, S. Lizano, L. Aguilar, and E. Daltabuit. Cambridge University Press, 145
Valera F., Aguilar L., Schuster W. 1994b, in Numerical Simulations in Astrophysics, eds. J. Franco, S. Lizano, L. Aguilar, and E. Daltabuit. Cambridge University Press, 111
Wisdom J. 1983, Icarus 56, 51
Wisdom J. 1987, Icarus 72, 241
Wisdom J., Peale S.J., Mignard F. 1984, Icarus 58, 137
Zinn R. 1985, ApJ 293, 424

This article was processed by the author using Springer-Verlag LaTeX A&A style file *L-AA* version 3.